SUPPLEMENTARY INFORMATION

Existence of long-lasting experience-dependent plasticity in endocrine cell networks

David J. Hodson[1,2,3*], Marie Schaeffer[1,2,3,4], Nicola Romanò[1,2,3], Pierre Fontanaud[1,2,3], Chrystel Lafont[1,2,3], Jerome Birkenstock[1,2,3], Francois Molino[1,2,3], Helen Christian[5], Joe Lockey[5], Danielle Carmignac[6], Marta Fernandez-Fuente[6], Paul Le Tissier[6] and Patrice Mollard[1,2,3*]

[1]CNRS, UMR-5203, Institut de Génomique Fonctionnelle, F-34000 Montpellier, France; [2]INSERM, U661, F-34000 Montpellier, France; [3]Universités de Montpellier 1 & 2, UMR-5203, F-34000 Montpellier, France; [4]Royal College of Surgeons in Ireland, Dublin 17, Ireland; [5]Department of Physiology, Anatomy and Genetics, University of Oxford, Oxford OX1 3QX, UK; [6]Division of Molecular Neuroendocrinology, MRC National Institute for Medical Research, Mill Hill, London NW7 1AA, UK.

[*]**Correspondence**:

David J. Hodson
Department of Endocrinology
Institut de Génomique Fonctionnelle
141, Rue de la Cardonille
34094 Montpellier CEDEX 05
France
e-mail: David.Hodson@igf.cnrs.fr
Tel: +33 (0)4 67 14 29 86
Fax: +33 (0)4 67 54 24 32

Patrice Mollard
Department of Endocrinology
Institut de Génomique Fonctionnelle
141, Rue de la Cardonille
34094 Montpellier CEDEX 05
France
e-mail: Patrice.Mollard@igf.cnrs.fr
Tel: +33 (0)4 34 35 92 70
Fax: +33 (0)4 67 54 24 32

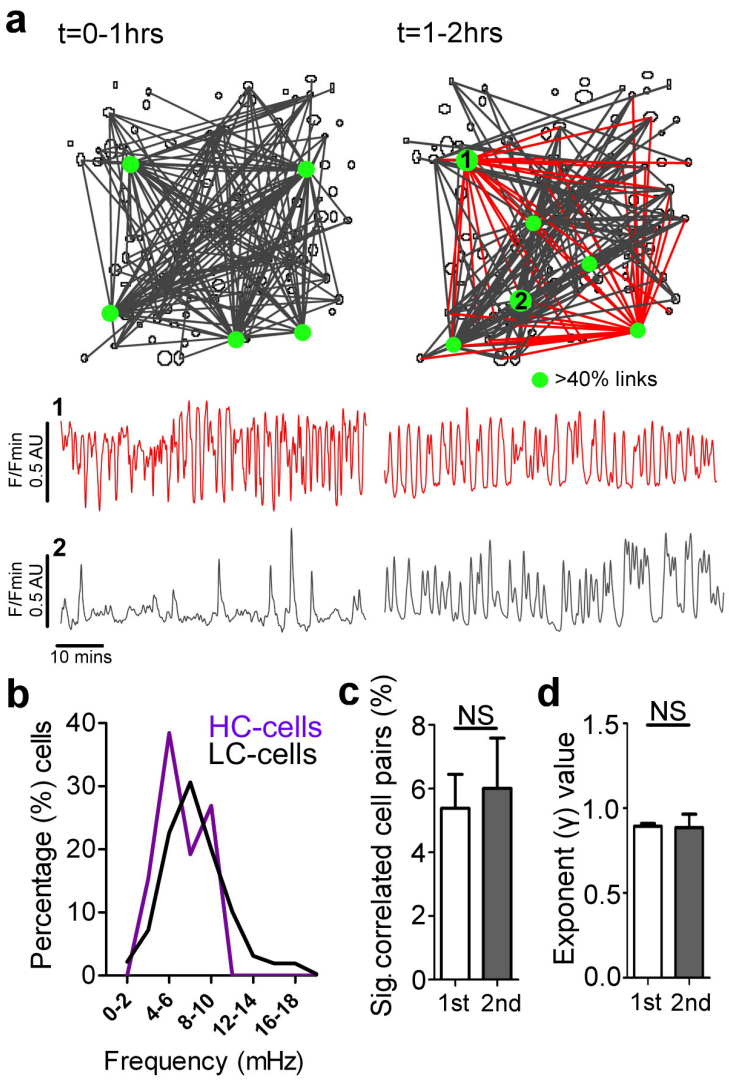

Supplementary Figure S1: Well-connected node cells are a dynamic feature of the lactotroph network due to Ca^{2+} spiking metastability. (a) Ca^{2+} signals were recorded from the lactotroph population of primiparas for one hour (t=0-1 hrs, left panel) (AU=arbitrary unit). Slices were then re-loaded with Ca^{2+}-indicator before re-commencing measurements of the same region for another hour (t=1-2 hrs, right panel). Highly-connected (HC) node cells (possessing >40 % of links) are marked in green. Note that, in this example, after a rest period of one hour, only 2 out of the original 5 node cells remain (links marked in red). However, high levels of connectivity are maintained by the appearance of node cells in new locations. The images are representative of 6 slices from 3 animals. (1) Cell no.1 (location marked as '1' on right functional connectivity map, panel a) is a cell that retained high levels of connectivity over both recording periods. Ca^{2+}-spiking activity is similar over the two periods. (2) Cell no. 2 (location marked '2' on right FC map, panel a) is a cell that was initially poorly connected but became highly connected during the second recording period. Ca^{2+}-activity shifted from single-spiking to plateauing. **(b)** Frequency (FFT) analysis of Ca^{2+} spikes emanating from lactotrophs of primipara slices reveals that activity of the highly-connected cells (>40% of links) is grouped into a similar frequency band compared to low connectivity (LC) cells (<40% of links) whose activity is more widely distributed across the power spectrum. Data represent the pooled values. **(c)** There is no difference in the percentage of significantly correlated cell pairs between the two recording periods (NS=non-significant vs. 1st period; Mann-Whitney U-test). Values represent mean ± S.E.M. **(d)** Exponent (γ) value (i.e. functional connectivity) is identical between the two recording periods (NS=non-significant vs. 1st period; Mann-Whitney U-test). Values represent mean ± S.E.M.

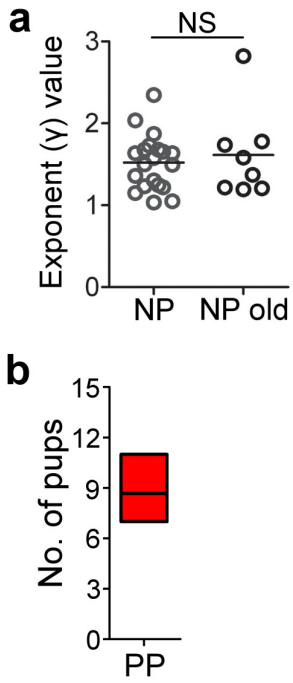

Supplementary Figure S2: Advancing age does not account for retention of a lactating-like FC following weaning and primiparas nurture on average 8 pups. (a) Connection distribution (i.e. mean power-law exponent; γ) was not significantly different in nulliparas (NP) compared to nulliparas of equivalent age to weaned dams (NP old) (NS=non-significant vs. NP) (n=8-20 slices). **(b)** Floating bar plot (displaying min-max values and median) of pup number in primiparas (n=24 litters).

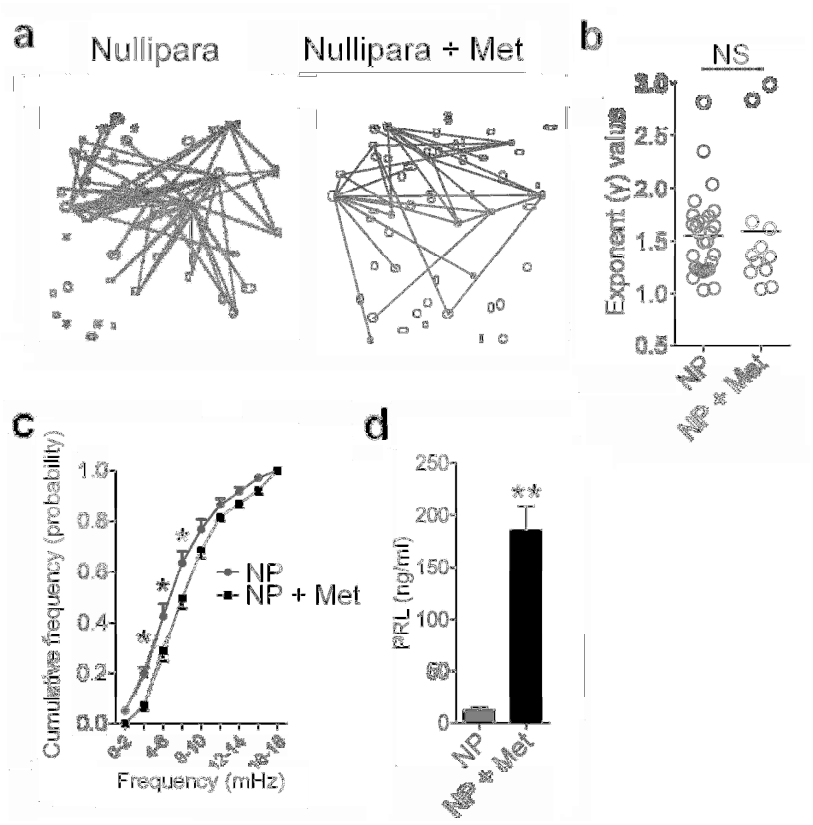

Supplementary Figure S3: Suckling is unlikely to evoke changes in functional connectivity through effects solely at the level of dopamine output. (a) No differences in functional connectivity (FC) patterns are apparent between control (NP) and treated nulliparas (NP + Met) following ten daily injections of metoclopramide (Met), a dopamine-2-receptor antagonist. **(b)** Scatter plot showing that metoclopramide is unable to significantly alter the mean exponent (γ) value and, hence, FC (NS = non-significant vs. NP + Met; Mann-Whitney U-test) (n=12-28 slices from at least 5 animals). **(c)** There is increased probability of cells displaying high frequency Ca^{2+}-spiking activity in the presence of metoclopramide as depicted using a cumulative frequency distribution (*P<0.05 vs. NP; two-way ANOVA) (n=11-18 slices from at least 5 animals). Values represent mean ± S.E.M. **(d)** Prolactin (PRL) concentrations following metoclopramide treatment are similar to those seen during lactation (**P<0.01 vs. NP; Mann-Whitney U-test) (n=6-19 animals). Values represent mean ± S.E.M.

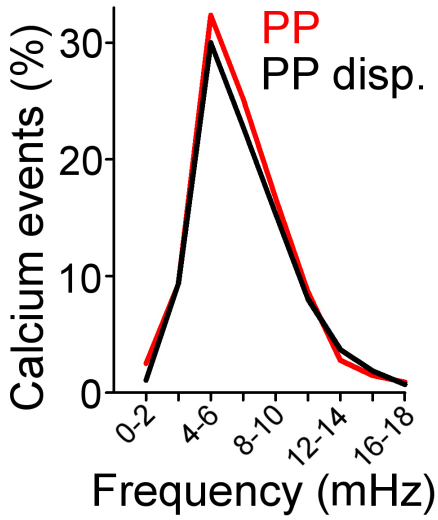

Supplementary Figure S4: Disruption of network architecture does not alter Ca^{2+}-spiking frequency. There is no difference in the distribution of Ca^{2+}-spiking frequencies between cells belonging to primipara slices (PP) and their enzymatically-dissociated counterparts (PP disp.) (two-way ANOVA) (n=8-18 recordings from at least 3 animals).

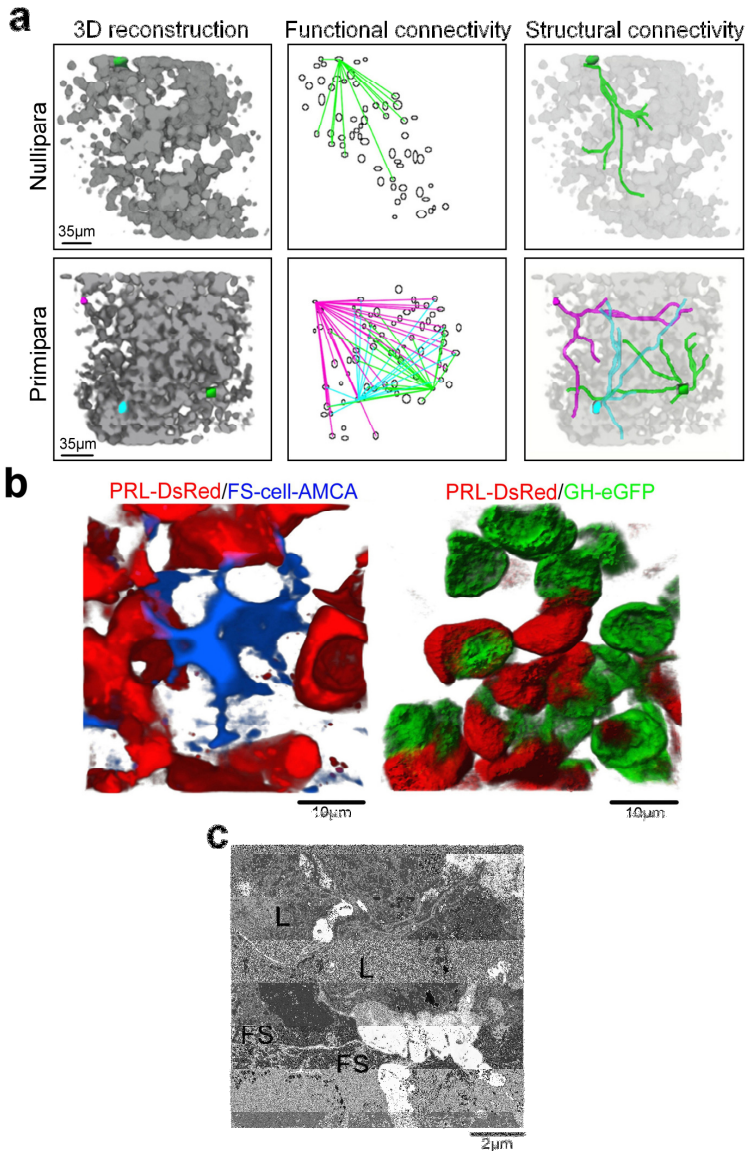

Supplementary Figure S5: Other pituitary cell types may also participate in functionally linking lactotrophs over long distances. (a) Functional- and structural- connectivity patterns are similar since nodes (highly connected cells; marked in color) are capable of directly contacting their correlated partners in three-dimensions through chains of structurally interconnected lactotrophs (grey). **(b)** Folliculostellate cells (FS-cell-AMCA; blue; left panel) and GH-cells (GH-eGFP; green; right panel) inter-link groups of lactotrophs (PRL-DsRed; red) and may act to convey information between distant regions of the lactotroph network. **(c)** Electron micrograph showing long processes of two folliculostellate cells (FS) making multiple junctional contacts with a lactotroph (L) in a nullipara.

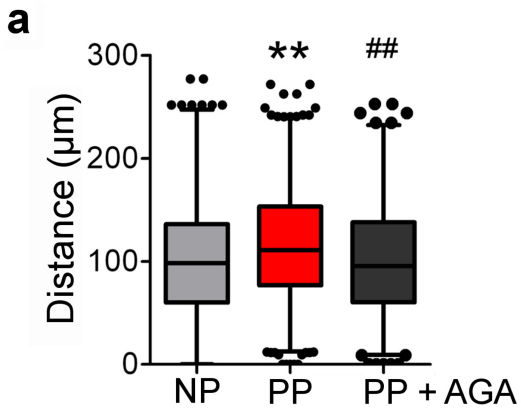

Supplementary Figure S6: Gap junction blockade reduces the average length between correlated cell pairs. Box and Whiskers plot (whiskers depict 1-99% percentile; outliers marked as circles) demonstrating an increase in average cell pair correlation length in primiparas (PP) vs. nulliparas (NP). Following application of 18-alpha-glycerrhitinic acid (AGA) to slices obtained from primiparas (PP + AGA), the distance between correlated cell pairs contracts by 15µm (**P<0.01 vs. NP, ##P<0.01 vs. PP; Kruskal-Wallis test) (n=7-18 slices from at least 5 animals).

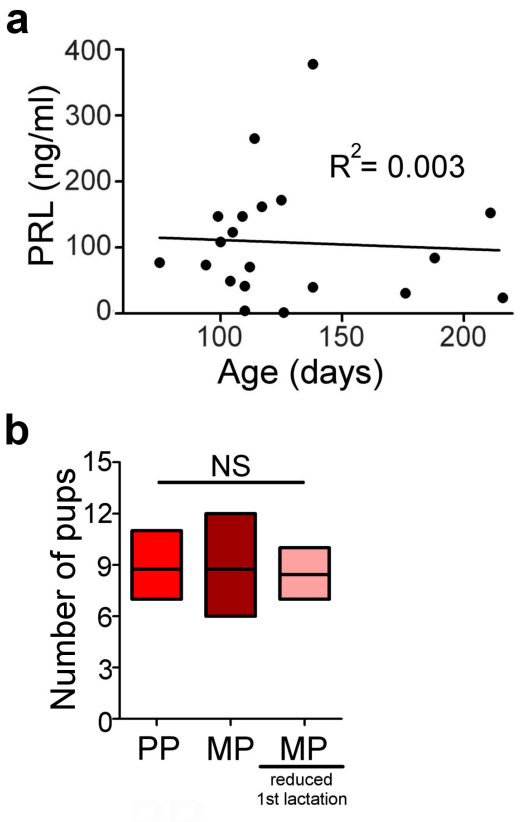

Supplementary Figure S7: Experience-dependent upregulation of hormone output is not due to age or altered suckling stimulus. (a) No linear relationship (R^2=0.003; linear regression analysis) is detected for age and prolactin (PRL) concentrations suggesting that the advancing age of multiparas (MP) versus primiparas (PP) does not play a role in the generation of higher levels of hormone secretion (n=20 animals). **(b)** Floating bar plot (displaying min-max values and median) showing that pup number is identical in primiparas, multiparas and multiparas subjected to reduced demand during the first lactation (NS = non-significant vs. PP; Kruskal-Wallis test) (n=7-24 litters).

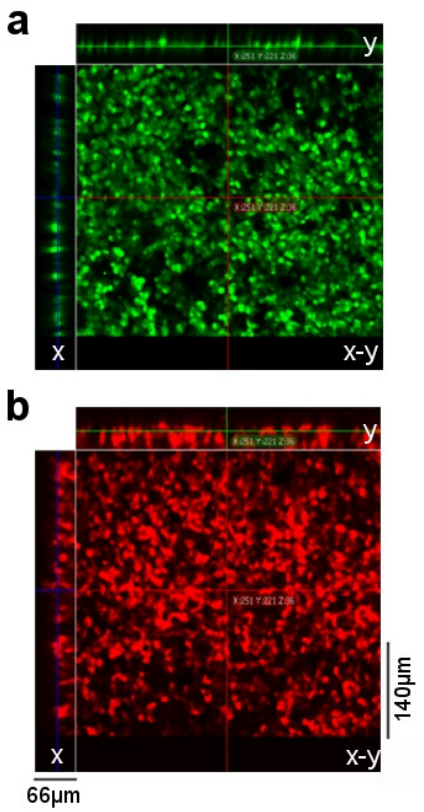

Supplementary Figure S8: Imaging fura-2 in acute pituitary slices. (a) 512x512µm xyz-projection of a pituitary slice incubated with fura-2-AM for 1 hr at 37˚C/5%CO_2. xz- and yz-projections are shown at the top and left side, respectively, of the xy-projection. Note that fura-2 is localised to the first and second cell layers. **(b)** As for (a) but xyz-projection of DsRed expression in the same pituitary slice. Note that DsRed expression is still readily detectable upto 40µm within the tissue, whereas fura-2 is absent at this depth.

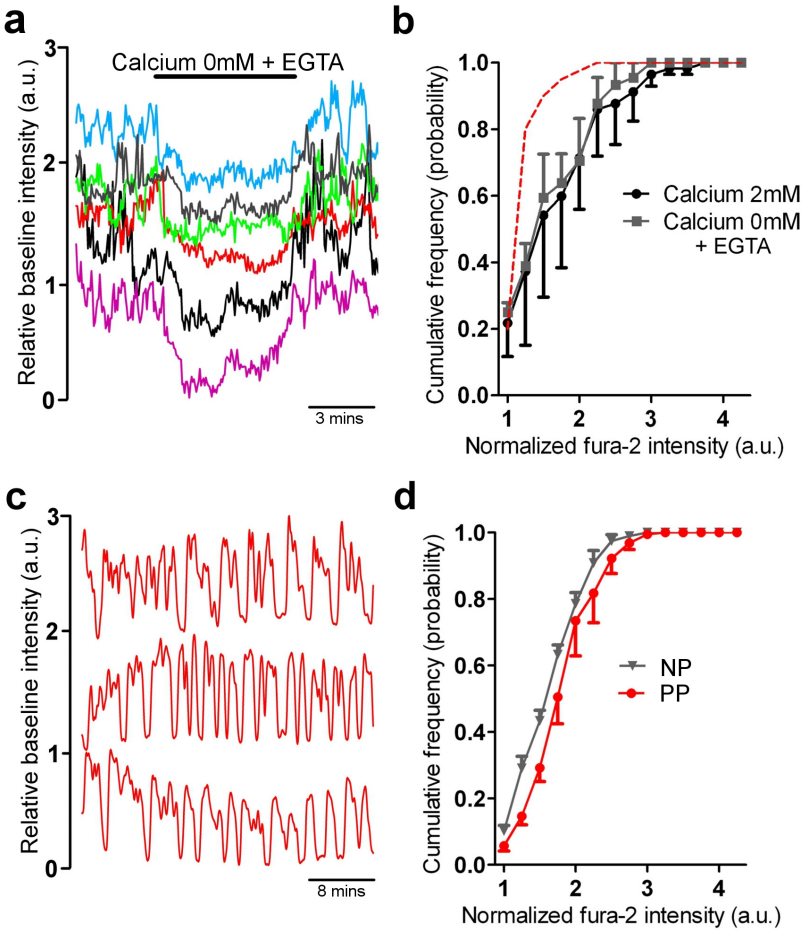

Supplementary Figure S9: Distribution of fura-2 loading does not alter intracellular calcium kinetics. (a) In nulliparas, cells respond to zero (0mM) Ca^{2+} + EGTA 5mM with decreases in intracellular Ca^{2+}-concentrations and fura-2 intensity. **(b)** The distribution of normalized intensity values are similar following application of normal (2mM) or Ca^{2+}-free Ringers (supplemented with EGTA) (two-way ANOVA) (n=3 animals). This suggests that discrepancies in fura-2 loading, as opposed to basal Ca^{2+} levels, account for the differences in baseline fluorescence. The dashed line (red) is the theoretical distribution of intensity values that would be expected if cell loading was similar but basal Ca^{2+} levels were different. Values represent mean ± S.E.M. **(c)** In primiparas, no changes in Ca^{2+}-spiking patterns are observed in cells differentially loaded with Ca^{2+}-indicator. **(d)** No significant differences in the distribution of fura-2 intensities are observed between the nullipara (NP) and primipara (PP) lactotroph population (two-way ANOVA) (n=4 animals). Values represent mean ± S.E.M.

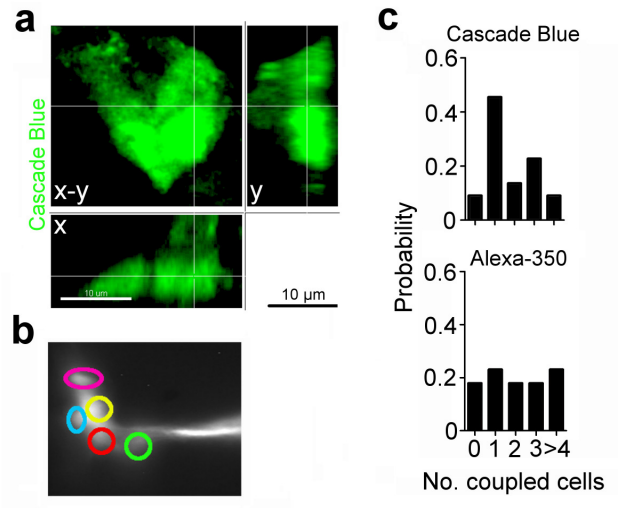

Supplementary Figure S10: Gap junction-coupling often involves cells in different focal planes, and no apparent changes in extent of diffusion are evident following dialysis with a lower molecular weight GJ-permeable dye. (a) Following injection of Cascade Blue into identified lactotrophs, slices were fixed in paraformaldehyde. Subsequent high-magnification confocal imaging demonstrates frequent transmission of Cascade Blue to lactotrophs in different planes (pseudo-coloured green). **(b)** Alexa-350, a lower molecular weight dye, diffuses to the same extent as Cascade Blue when injected into lactotrophs. **(c)** Histograms showing probability of cell coupling in slices from weaned animals micro-injected with Cascade Blue (top panel) (n=25) and Alexa-350 (bottom panel) (n=21).

SUPPLEMENTARY METHODS

Drug treatment

To investigate the effects of dopamine tone on lactotroph network connectivity, virgin DsRed animals received daily injections of metoclopramide (7.5mg/kg) (a specific D2-antagonist). To ensure high basal levels of PRL, 50mg/l of the same compound was placed in the drinking water supplemented with sucrose (0.5%) to increase palatability. Animals were treated for 10 days, sacrificed either immediately or 3 weeks later, and pituitary glands prepared as described. Plasma was retained for measurement of PRL concentrations to confirm efficacy of treatment.

Cell dispersion

Adenohypophyses (with the pars intermedia and nervosa removed) were pre-incubated for 10 minutes in trypsin (0.05%) before trituration and dispersion for 25 minutes in HBSS pH 7.4 containing dispase (50 caseinolytic units/ml) (BD Bioscience, France), collagenase A (2.25mg/ml) and DNAase (25µg/ml) (all from Sigma-Aldrich). Cells were plated at high density on coverslips coated with Poly-D-lysine (0.1%) (BD Bioscience).

Multiphoton and confocal imaging of fixed tissue

Folliculostellate cells were specifically labelled by pre-incubating live tissue in β-Ala-Lys-Nε-*AMCA* (40µM) (BioTrend, Switzerland) for 1.5 hour at 37˚C before fixation[1]. Tissues were imaged using Zeiss LSM510 multiphoton and meta-confocal systems (Carl Zeiss AG, Jena, Germany). For the former, excitation was delivered at 880nm and emitted signals were recorded from 500-550nm for eGFP and 576-661nm for DsRed in multi-track mode. For the latter, emitted signals were captured from 585-615nm for DsRed (excitation 543nm) and 420-480nm for AMCA (excitation 405nm) in single-track mode. Both low (10x EC Plan-Neofluar, NA 0.3, Zeiss) and high (40x, NA 1.3, Plan Apochromat, Zeiss) magnification objectives were used. Network and individual cell volumes were calculated from the 3D-stacks using the surface rendering tool in Imaris (Bitplane, Zurich, Switzerland).

Correlation analysis

Ca^{2+} time-lapse movies were constructed using ImageJ. Cells positive for both fura-2 and DsRed were identified by a region of interest and fluorescence intensity over time measurements obtained. As deflections in fura-2 emission intensity corresponded to rises in cytosolic Ca^{2+} (fura-2 excitation above the isosbestic point), fluorescence emission signals

were inverted. Ca^{2+} traces were then normalized (F/F_{min}) and manually checked to ensure the following: absence of erratic fluctuations in baseline fluorescence; sustained spiking activity at least 2-fold greater than the CCD readout noise level (practically all cells were spontaneously active under all conditions examined); and absence of artefacts such as rapid and sustained increases in cytosolic Ca^{2+}-concentrations indicative of cell death. Approximately one-quarter of cells were excluded from subsequent analysis.

Cell-cell correlation analyses were performed using custom software programmed in MATLAB (Mathworks, MA, USA) (code available upon request). Since correlation analyses assumes a stable baseline, Ca^{2+} traces were subjected to Huang-Hilbert type empirical mode decomposition (perso.ens-lyon.fr/patrick.flandrin/emd.html) to retrieve the baseline trend and account for artefacts such as photobleaching. Subsequently, activity profiles were binarized such that, at each time point, cells with a deflection above the de-trended baseline were considered as being 'on' and represented with a '1' whereas inactivity was represented as '0'. For each cell, a 20% threshold was imposed to avoid false detection of signals emanating from residual fluctuations in baseline fluorescence. Due to the spectral properties of fura-2 under multi-photon excitation, Ca^{2+} spike amplitude tended to be artificially compressed as resting fluorescence (F_{min}) declined over time as a consequence of photobleaching/dye leakage. Therefore, to prevent erroneous shortening of 'on periods', Ca^{2+} signals were de-compressed using a normalized cumulative distribution frequency to equalize the histogram for each image in the sequence. Following signal binarization, population activity was represented as a raster plot and correlations of activity measured as:

$$Ci\,j = \frac{T\,ij}{\sqrt{T\,i\,T\,j}} \quad \text{(S1)}$$

where T_{ij} is the total coactivity time and T_i and T_j are the total activity time for the two cells considered. Following analysis of the Ca^{2+} traces, a correlation matrix for all the cell pairs was constructed, and the significance of the measured correlations assessed versus chance by subjecting the activity events of each cell to Monte Carlo shuffling. Using the significant correlations, a weighted graph displaying the distribution of connections (k) between nodes (n) was constructed, allowing the cell network to be depicted as detailed in (*23*). Subsequently, probability was plotted as a function of connection number and a power law function, $f(x) = ax^k + o(x^k)$, fitted to the resulting points using EzyFit 2.4 toolbox for MATLAB (http://www.fast.u-psud.fr/ezyfit/). Goodness of fit was determined using MATLAB's inbuilt Nelder-Mead method.

To assess synchronized Ca^{2+}-spiking behavior, the coactivity (%) for each experiment was calculated using the binarized cell activity dataset. Subsequently, inter-coactivity intervals were assessed by differentiating the number of events surpassing a 95% significance threshold. To filter signal jitter arising at intervals close to the acquisition rate, pooled histograms were constructed using a starting bin of 15 seconds (i.e. 2 x the Nyquist frequency). The degree of dispersion around the geometric mean was determined by fitting a Gaussian curve.

Connectivity analysis

3D reconstructions of the region of the lactotroph network subjected to Ca^{2+} -imaging were generated for each experiment. The images were binarized, and non-connected objects removed since connectivity analysis assumes that there is only a single foreground particle and no cavities in the image. To obtain a representative number of connected objects for each experiment, a custom algorithm was written for Matlab which performed multiple iterations on each z-stack to segregate connected objects comprising at least 20% of the total pixel number. Using the Euler characteristic ($\chi = V - E + F$, where V, E and F are the numbers of vertices, edges and faces, respectively), the connectivity, β, of each sample was calculated in a manner which excluded finite volume sampling effects ($\beta = 1 - \Delta\chi$, where $\Delta\chi$ accounts for the intersection of the structure with the boundaries of the stack). Thus, a high value for β indicates a high degree of voxel interconnectedness. BoneJ plugin for ImageJ was used to binarise images and analyse connectivity (Doube M (2010) BoneJ v1.1.9 http://bonej.org/). The Euler characteristic was deemed to be most suitable for structural connectivity analysis since it allows the number of connected structures to be calculated irrespectively of the manner in which the structure occupies space. Paths of homotypically-connected lactotrophs were traced in three-dimensions using stacks acquired of the area subjected to Ca^{2+}-imaging and Simple Neurite Tracer plugin (http://www.longair.net/edinburgh/imagej/tracer/) for Fiji (http://pacific.mpi-cbg.de/wiki/index.php/Fiji).

Frequency analysis

Ca^{2+}-spiking frequency was measured using the Fourier transform. Power spectrums were constructed for each cell in the population and the frequency with the greatest power (above a 95% confidence interval) extracted. For each experiment, histograms of frequency (mHz) were plotted (binning 2mHz) and data compared between states.

Supplementary Reference

30 Fauquier, T., Guerineau, N. C., McKinney, R. A., Bauer, K. & Mollard, P. Folliculostellate cell network: a route for long-distance communication in the anterior pituitary. *Proc. Natl. Acad. Sci. U. S. A.* 98, 8891-8896 (2001).